JHEP

Published for SISSA by Springer

Received: November 23, 2016
Revised: January 16, 2017
Accepted: February 6, 2017
Published: February 16, 2017

Single-diffractive production of charmed mesons at the LHC within the k_t-factorization approach

Marta Łuszczak,[a] **Rafał Maciuła,**[b] **Antoni Szczurek**[b,1] **and Maciej Trzebiński**[b]

[a] *University of Rzeszów, PL-35-959 Rzeszów, Poland*
[b] *Institute of Nuclear Physics PAN, PL-31-342 Cracow, Poland*

E-mail: luszczak@univ.rzeszow.pl, rafal.maciula@ifj.edu.pl, antoni.szczurek@ifj.edu.pl, maciej.trzebinski@ifj.edu.pl

Abstract: We discuss the single-diffractive production of $c\bar{c}$ pairs and charmed mesons at the LHC. For a first time we propose a k_t-factorization approach to the diffractive processes. The transverse momentum dependent diffractive parton distributions are obtained from standard (collinear) diffractive parton distributions used in the literature. In this calculation the transverse momentum of the pomeron is neglected with respect to transverse momentum of partons entering the hard process. We also perform a first evaluation of the cross sections at the LHC using the diffractive transverse momentum dependent parton distributions. The results of the new approach are compared with those of the standard collinear one. Significantly larger cross sections are obtained in the k_t-factorization approach in which some parts of higher-order effects is effectively included. The differences between corresponding differential distributions are discussed. Finally, we present a feasibility study of the process at the LHC using proton tagging technique. The analysis suggests that the measurement of single-diffractive charm production is possible using ATLAS and CMS/TOTEM detectors.

Keywords: QCD Phenomenology, Phenomenological Models

ArXiv ePrint: 1606.06528

[1] Also at University of Rzeszów, PL-35-959 Rzeszów, Poland.

Open Access, © The Authors.
Article funded by SCOAP[3].

doi:10.1007/JHEP02(2017)089

Contents

JHEP02(2017)089

1 Introduction

Diffractive hadronic processes are a special class of production mechanisms when forward emitted proton(s) is (are) accompanied by a sizeable (a few rapidity units) rapidity gap(s) starting from the most forward (in rapidity) proton(s) towards midrapidities. If only one of the forward protons is required, such processes are called single-diffractive. These processes were studied theoretically in the so-called resolved pomeron model [1]. It was realized during the Tevatron runs that the model, previously used to describe deep-inelastic diffractive processes, must be corrected to take into account absorption effects related to hadron-hadron interactions. Such interactions, unavoidably present in hadronic collisions at high energies and not present in electron/positron induced processes, lead to a damping of the diffractive cross section. In theoretical models this effect is taken into account by multiplying the diffractive cross section calculated using HERA diffractive PDFs by a phase-space independent factor called the gap survival probability — S_G. Two theoretical groups specialize in calculating such probabilities [2–4] and provide numerical values of S_G for various energies and different types of diffractive mechanisms. At high energies such factors, interpreted as probabilities, are very small (of the order of a few %). This causes that the predictions of the diffractive cross sections are not as precise as those for the standard inclusive non-diffractive cases. This may become a challenge after a precise diffractive data from the LHC will become available.

Several processes have been considered on the theoretical side and discussed in the literature. Studies were performed for single W [5, 6] and Z [7] boson, di-jet [8], direct photon [9], photon-jet [10], di-lepton [11, 12], W^+W^- [13], $c\bar{c}$ [14] and $b\bar{b}$ [15] pair production. This list in not complete and other processes are also possible.

From the experimental side there are also several interesting results published. For example: rapidity cross sections [16], production of diffractive minimum-bias [17, 18], production of W bosons [19, 20] and di-jets [21–24].

There are two alternative approaches in the literature how to calculate hard-diffractive processes. In the so-called dipole approach the amplitudes are modeled using a phenomenological ingredient: dipole-proton interaction cross section which is fitted to HERA data. The dipole model by construction violates Regge factorization. In ref. [25] an extra absorption was added on the top of the dipole model result. Recently we have carefully discussed several weak points of the dipole approach for the inclusive Drell-Yan processes [26].

The published paper on single-diffractive production of $c\bar{c}$ [25] includes only processes that avoid so-called pomeron remnants in the final state. In contrast, only the latter ones are included in the resolved pomeron model.

The resolved pomeron model, the one we are using here, is constructed according to quite different philosophy based on the so-called diffractive parton distributions. The latter objects are constructed based on the Regge picture but are adjusted to experimental data measured at HERA. This approach is commonly accepted in the literature. It was commonly used for different single-diffractive processes (dijets, $q\bar{q}$, W, Z, photon-jet, Drell-Yan). Using naively the model with parameter from HERA at hadronic processes would be consistent with factorization. In our model factorization is, however, broken by absorption corrections included explicitly in our calculation.

In ref. [27] we have discussed a formally equivalent (to the dipole approach) approach where we use unintegrated gluon distributions instead of parametrizing dipole cross section. The cross section obtained in this approach is, however, much smaller than the cross section obtained in the present paper. This was interpreted in ref. [27] as being only a small, semi-exclusive contribution to the diffractive $c\bar{c}$ cross section, so cannot replace the resolved contribution with pomeron remnant in the final state. In addition, this is a mechanism which corresponds to a mechanism considered in the dipole model.

In this paper we consider diffractive production of charm for which rather large cross section at the LHC are expected, even within the leading-order (LO) collinear approach [28]. On the other hand, it was shown that for the inclusive non-diffractive charm production the LO collinear approach is rather poor approximation and higher-order corrections are crucial. In contrast, the k_t-factorization approach, which effectively includes higher-order effects, gives a good description of the LHC data for inclusive charm production at $\sqrt{s}$ = 7 TeV (see e.g. ref. [29]). This strongly suggests that application of the k_t-factorization approach to diffractive charm production would be useful.

To sum up, the measurement of diffractive production of charm would be very useful to pin down the mechanism of diffractive production in general. Since such a measurement seems important and useful, in the present paper we present also a feasibility study for the diffractive production of charm mesons within the ATLAS and CMS/TOTEM detectors. Experimentally, diffractive events could be selected by looking for the large rapidity gaps or by measuring the forward protons that remain intact during the interactions. The latter formally requires a cooperation of the main ATLAS or CMS detectors with a special dedicated forward detectors being installed.

JHEP02(2017)089

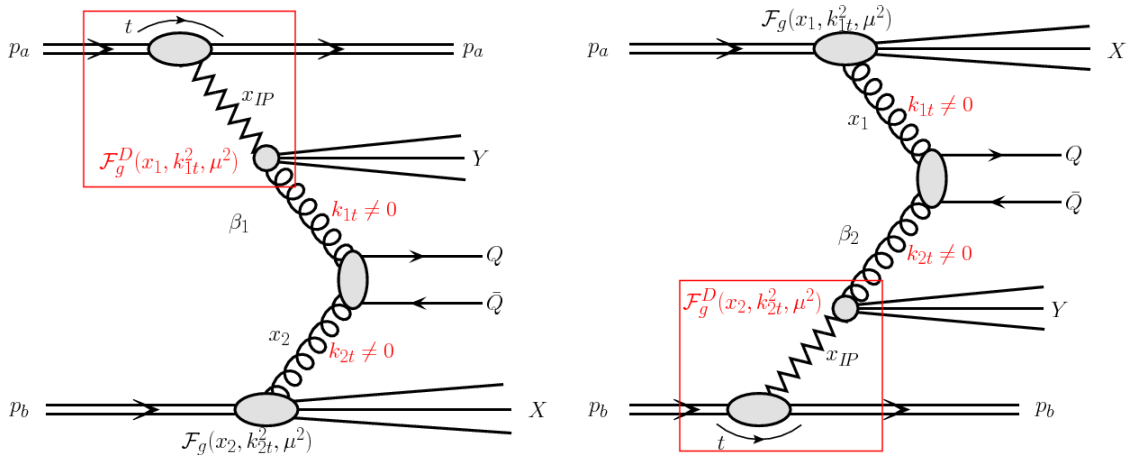

Figure 1. A diagrammatic representation of the considered mechanisms of single-diffractive production of heavy quark pairs within the k_t-factorization approach.

The present paper is organized as follows. Section 2 describes the theoretical framework based on the so-called resolved pomeron model extended to the k_T-factorization formalism that is used in the numerical calculations throuhout the whole paper. In section 3 we present first numerical results of the calculations of the single-diffractive cross section for charm quarks and for D mesons at the LHC, including several differential single-particle as well as correlation distributions. Section 4 is devoted to the discussion of the role of the gap survival factor, its contribution to the overall uncertainty of the theoretical predictions and its possible extension to the phase-space dependent version in future. Section 5 contains detailed feasibility studies of the process under consideration, that are especially focused on the ATLAS and/or CMS future analyses. Finally, some concluding remarks and outlook are given in section 6.

2 Formalism

A sketch of the underlying mechanism with the notation of kinematical variables or some theoretical ingredients used in the theoretical formalism is shown in figure 1. Here, we propose an extension of the standard resolved pomeron model [1] based on the LO collinear approach by adopting a framework of the k_t-factorization as an effective way to include higher-order corrections. Such an approach is very useful e.g. in the studies of kinematical correlations [29]. According to this model the cross section for a single-diffractive production of charm quark-antiquark pairs, for both considered diagrams (left and right panel of figure 1), can be written as:

$$d\sigma^{SD(a)}(p_a p_b \to p_a c\bar{c}\, XY) = \int dx_1 \frac{d^2k_{1t}}{\pi} dx_2 \frac{d^2k_{2t}}{\pi}\, d\hat{\sigma}(g^* g^* \to c\bar{c}) \times \mathcal{F}_g^D(x_1, k_{1t}^2, \mu^2) \cdot \mathcal{F}_g(x_2, k_{2t}^2, \mu^2), \tag{2.1}$$

$$d\sigma^{SD(b)}(p_a p_b \to c\bar{c} p_b\, XY) = \int dx_1 \frac{d^2k_{1t}}{\pi} dx_2 \frac{d^2k_{2t}}{\pi}\, d\hat{\sigma}(g^* g^* \to c\bar{c}) \times \mathcal{F}_g(x_1, k_{1t}^2, \mu^2) \cdot \mathcal{F}_g^D(x_2, k_{2t}^2, \mu^2), \tag{2.2}$$

JHEP02(2017)089

where $\mathcal{F}_g(x,k_t^2,\mu^2)$ are the "conventional" unintegrated (k_t-dependent) gluon distributions (UGDFs) in the proton and $\mathcal{F}_g^D(x,k_t^2,\mu^2)$ are their diffractive counterparts — which we will call here diffractive UGDFs (dUGDFs). The latter can be interpreted as a probability of finding a gluon with longitudinal momentum fraction x and transverse momentum (virtuality) k_t at the factorization scale μ^2 assuming that the proton which lost a momentum fraction x_{IP} remains intact.

In the approach applied here, we neglect a possible influence of the pomeron/reggeon transverse momentum on the transverse momentum of the initial off-shell gluon from pomeron/reggeon. The effect is assumed to be negligible since the transverse momenta of incident gluon are typically larger (or much larger) than the transverse momenta of pomeron/reggeon (equal to the transverse momenta of outgoing proton). We will come back to the issue when presenting numerical results.

The partonic cross section for the considered hard scattering reads:

$$d\hat{\sigma}(g^*g^* \to c\bar{c}) = \frac{d^3p_1}{2E_1(2\pi)^3}\frac{d^3p_2}{2E_2(2\pi)^3}(2\pi)^2\delta^2(p_1+p_2-k_1-k_2) \times \overline{|\mathcal{M}_{g^*g^*\to c\bar{c}}(k_1,k_2)|^2}\,, \tag{2.3}$$

where p_1, E_1 and p_2, E_2 are the momenta and energies of outgoing c and $\bar{c}$, respectively, and $\overline{|\mathcal{M}_{g^*g^*\to c\bar{c}}(k_1,k_2)|^2}$ is the off-shell matrix element for the $g^*g^* \to c\bar{c}$ sub-process.

According to the so-called proton-vertex factorization, the diffractive collinear gluon distribution in the proton can be written in the form where the variables related to the proton kinematics are separated from those connected with the hard interaction:

$$g^D(x,\mu^2) = \int dx_{IP} d\beta\, \delta(x - x_{IP}\beta) g_{IP}(\beta,\mu^2)\, f_{IP}(x_{IP}) = \int_x^{x^{\max}} \frac{dx_{IP}}{x_{IP}}\, f_{IP}(x_{IP}) g_{IP}\left(\frac{x}{x_{IP}},\mu^2\right), \tag{2.4}$$

where $\beta = \frac{x}{x_{IP}}$ is the longitudinal momentum fraction of the pomeron carried by gluon and the flux of pomerons may be taken as:

$$f_{IP}(x_{IP}) = \int_{t_{\min}}^{t_{\max}} dt\, f(x_{IP},t). \tag{2.5}$$

The unintegrated (k_t-dependent) diffractive gluon distributions in the proton can be easily obtained from the collinear diffractive PDFs by applying the Kimber-Martin-Ryskin (KMR) approach [30]. According to this procedure, the diffractive unintegrated gluon distribution is given by the following formula:

$$f_g^D(x,k_t^2,\mu^2) \equiv \frac{\partial}{\partial \log k_t^2}\left[\, g^D(x,k_t^2)\, T_g(k_t^2,\mu^2)\,\right] = T_g(k_t^2,\mu^2)\,\frac{\alpha_S(k_t^2)}{2\pi} \times \int_x^1 dz \left[\sum_q P_{gq}(z)\frac{x}{z}\, q^D\left(\frac{x}{z},k_t^2\right) + P_{gg}(z)\frac{x}{z}\, g^D\left(\frac{x}{z},k_t^2\right)\Theta\left(\Delta - z\right)\right], \tag{2.6}$$

where g^D and q^D are the collinear diffractive PDFs in the proton and can be taken e.g. from the H1 Collaboration analysis of diffractive dijets and diffractive structure function [31].

JHEP02(2017)089

The P_{gq} and P_{gg} are the usual unregulated LO DGLAP splitting functions. The Heaviside step function Θ implies the angular-ordering constraint of the phase space $\Delta = \mu/(\mu + k_t)$ for gluon emission particularly to the last evolution step to regulate the soft gluon singularities. The above definition is fully satisfied for $k_t > \mu_0$, where $\mu_0 \sim 1\,\text{GeV}$ is the minimum scale for which DGLAP evolution of the collinear diffractive PDFs is valid. The Sudakov form factor $T_g(k_t^2, \mu^2)$ is responsible for virtual loop corrections and gives the probability of evolving from a scale k_t to a scale μ without any new parton emissions. It may be written in the simplified form as:

$$T_g(k_t^2, \mu^2) = \exp\left(- \int_{k_t^2}^{\mu^2} \frac{\mathrm{d}\kappa_t^2}{\kappa_t^2} \frac{\alpha_S(\kappa_t^2)}{2\pi} \left(\int_0^{1-\Delta} \mathrm{d}z\, z P_{gg}(z) + n_F \int_0^1 \mathrm{d}z\, P_{qg}(z) \right) \right), \quad (2.7)$$

where n_F is the number of quark-antiquark flavours into which the gluon may split. Due to the presence of the Sudakov form factor in the KMR prescription only last emission generates transverse momentum of the incoming gluons. The unique feature of the KMR model of UGDF is providing possibility for the emission of at most one additional gluon. Therefore, one can expect that the KMR model may include in an effective way higher-order corrections to heavy quark production cross section.

Because of the UGDF definition in the KMR approach one needs to also apply the following transformation:

$$\mathcal{F}_g^D(x, k_t^2, \mu^2) \equiv \frac{1}{k_t^2} f_g^D(x, k_t^2, \mu^2)\,. \quad (2.8)$$

Then the normalisation condition for diffractive unintegrated gluon distribution:

$$g^D(x, \mu^2) = \int_0^{\mu^2} dk_t^2\, f_g^D(x, k_t^2, \mu^2), \quad (2.9)$$

is exactly satisfied if one defines:

$$\mathcal{F}_g^D(x, k_t^2, \mu^2)\big|_{k_t < \mu_0} = \frac{1}{\mu_0^2} g^D(x, \mu_0^2)\, T_g(\mu_0^2, \mu^2), \quad (2.10)$$

so that the density of gluons in proton is constant for $k_t < \mu_0$ at fixed x and μ.

In this paper, the diffractive KMR UGDFs are calculated from the "H1 2006 fit A" diffractive collinear PDFs [31], that are only available at next-to-leading order (NLO). Consistently, in the calculation of the conventional non-diffractive KMR UGDFs the MSTW2008nlo collinear PDFs [32] were used. In the perturbative part of calculations we take running coupling constant $\alpha_S(\mu_R^2)$, the charm quark mass $m_c = 1.5\,\text{GeV}$ and the renormalization and factorization scales equal to the transverse mass of charm quarks/antiquarks $\mu^2 = \mu_R^2 = \mu_F^2 = \frac{m_{1t}^2 + m_{1t}^2}{2}$, where $m_t = \sqrt{p_t^2 + m_c^2}$.

3 First numerical results

A naive application of Regge factorization to hadron-hadron collisions is known to be violated. This is due to the fact that soft interactions lead to an extra production of particles which fill the rapidity gaps related to pomeron/reggeon exchange. Therefore, in

JHEP02(2017)089

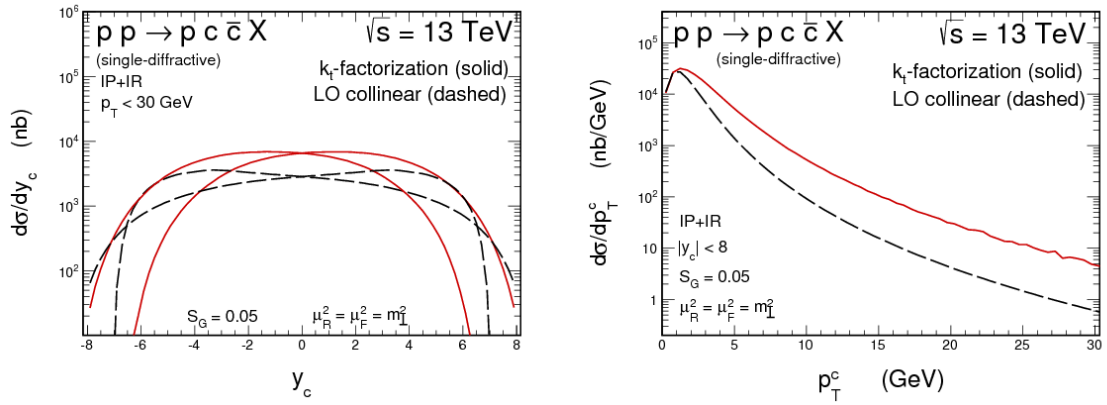

Figure 2. Rapidity (left panel) and transverse momentum (right panel) distributions of c quarks (antiquarks) for a single-diffractive production at $\sqrt{s} = 13\,\text{TeV}$. Components of the $g(IP)$ - $g(p)$, $g(p)$ - $g(IP)$, $g(IR)$ - $g(p)$, $g(p)$ - $g(IR)$ mechanisms are included. Results for the LO collinear (black long-dashed) and the k_t-factorization approach (red solid) are shown separately. Details are specified in the figure legends.

the calculations below we use the gap survival probability factor $S_G = 0.05$ (used by other authors) to effectively include these effects. This is very approximate approach. We expect related uncertainty of the order of factor 2. Clearly dedicated studies are required in future. Some aspects of the problem are discussed in section 4, some are left for future studies.

In figure 2 we show rapidity (left panel) and transverse momentum (right panel) distribution of c quarks (antiquarks) for the single diffractive production at $\sqrt{s} = 13\,\text{TeV}$ in proton-proton scattering. The leading $g(IP)$ - $g(p)$, i.e. gluon in pomeron – gluon in proton, (or $g(p)$ - $g(IP)$) and the subleading $g(IR)$ - $g(p)$, i.e. gluon in reggeon – gluon in proton, (or $g(p)$ - $g(IR)$) components are included. We limit the range of the momentum fractions x_{IP} and x_{IR} in the numerical calculations to $x_{IP}, x_{IR} < 0.15$ which reflects the maximal experimental coverage at the LHC.

Distributions calculated within the LO collinear factorization (black long-dashed lines) and for the k_t-factorization approach (red solid lines) are shown separately. We see significant differences between the both approaches, which are consistent with similar studies of standard non-diffractive charm production (see e.g. ref. [29]). Here we confirm that the higher-order corrections are very important also for the diffractive production of charm quarks. Predictions within the k_t-factorization give a significantly larger differential cross section in the whole p_t and y ranges, except for a very small transverse momenta and extremely forward/backward rapidities.

In figure 3 we show the invariant mass distribution of $c\bar{c}$ pairs for a single-diffractive production at $\sqrt{s} = 13\,\text{TeV}$. The shapes of the distributions obtained for the LO collinear and the k_t-factorization approach are rather similar. However, the latter gives larger cross section approximately by a factor of almost 2–3.

Figure 4 shows the differential cross section as a function of $\log_{10}(x)$ where x is defined as the longitudinal momentum fraction of proton carried by the gluon from non-diffractive

JHEP02(2017)089

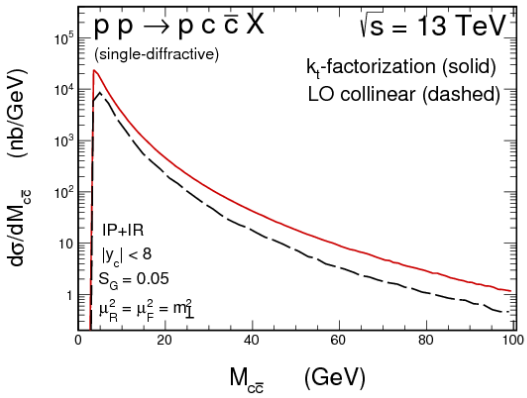

Figure 3. Invariant mass distributions of $c\bar{c}$ pairs for a single-diffractive production at $\sqrt{s} = 13\,\text{TeV}$. Here, the charm quark rapidity and transverse momentum were limited to $|y| < 8$ and $0 < p_t < 30\,\text{GeV}$, respectively.

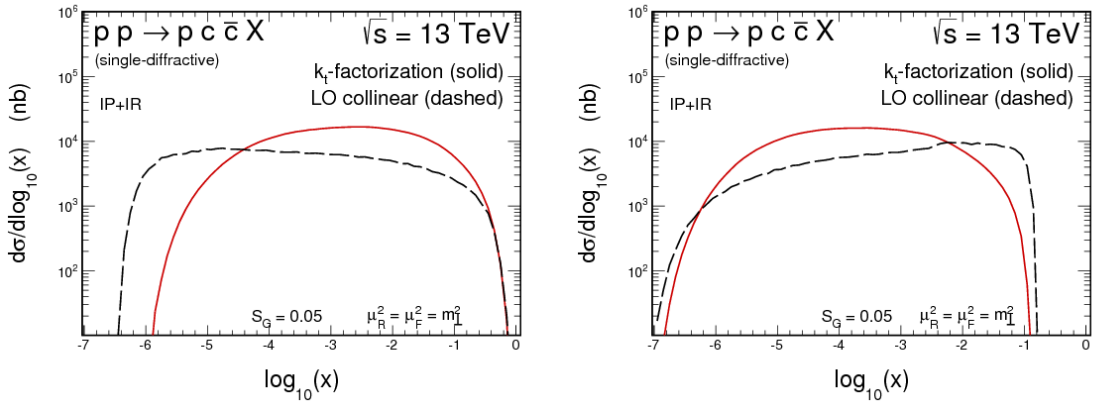

Figure 4. The differential cross section as a function of $\log_{10}(x)$ with x being the non-diffractive gluon longitudinal momentum fraction (left panel) and the diffractive gluon longitudinal momentum fraction with respect to the proton (right panel) for single-diffractive production at $\sqrt{s} = 13\,\text{TeV}$. Results for the LO collinear (black long-dashed) and the k_t-factorization (red solid) approaches are compared.

side (left panel) or as the longitudinal momentum fraction of proton carried by the diffractive gluon emitted from pomeron/reggeon on diffractive side (right panel). In the case of non-diffractive gluon (left panel) we see that for extremely small x values the LO collinear predictions strongly exceed the ones of the k_t-factorization. This effect also affects the rapidity spectra in the very forward/backward regions (see figure 2) and is partially related to a very poor theoretical control of the collinear PDFs in the range of x below 10^{-5}.

In figure 5 we show again the rapidity (left panel) and transverse momentum (right panel) distributions of c quarks (antiquarks) calculated in the k_t-factorization approach. Here contributions from the pomeron and the reggeon exchanges are shown separately. The estimated sub-leading reggeon contribution is of similar size as the one of the leading pomeron. In the single-diffractive case the maxima of rapidity distributions for $g(IP)$ - $g(p)$

JHEP02(2017)089

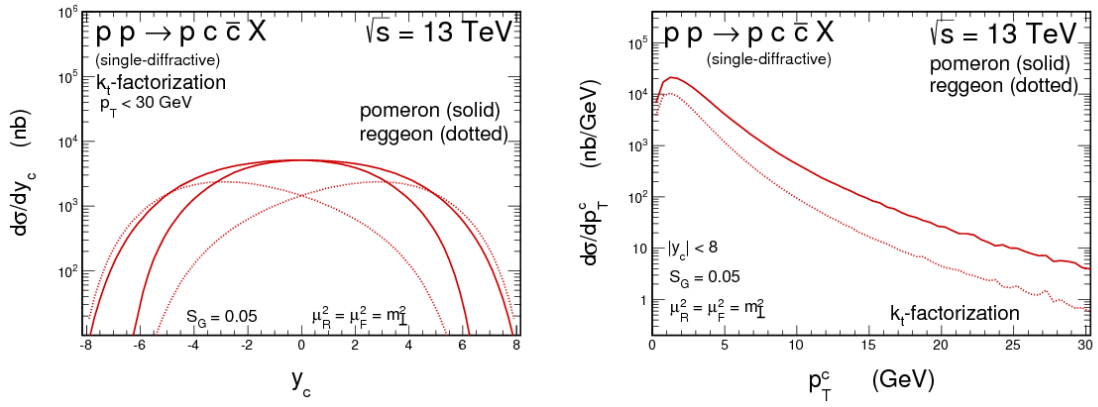

Figure 5. Rapidity (left panel) and transverse momentum (right panel) distributions of c quarks (antiquarks) for single-diffractive production at $\sqrt{s} = 13\,\text{TeV}$ calculated within the k_t-factorization approach. Contributions of the $g(IP)$ - $g(p)$, $g(p)$ - $g(IP)$, $g(IR)$ - $g(p)$, $g(p)$ - $g(IR)$ mechanisms are shown separately.

and $g(p)$ - $g(IP)$ (or $g(IR)$ - $g(p)$ and $g(p)$ - $g(IR)$) mechanisms are shifted to forward and backward rapidities with respect to the non-diffractive case. This is related to the upper limit on diffractive gluon longitudinal momentum fraction ($x \leq x_{IP}$).

Now we start our presentation of correlation observables. They cannot be calculated within the LO collinear factorization but are easily obtainable in the k_t-factorization approach.

The distribution of azimuthal angle $\varphi_{c\bar{c}}$ between c quarks and $\bar{c}$ antiquarks is shown in the left panel of figure 6. The $c\bar{c}$ pair transverse momentum distribution $p_T^{c\bar{c}} = |\vec{p}_t^{\,c} + \vec{p}_t^{\,\bar{c}}|$ is shown in the right panel. The results of the full phase-space calculations illustrate that the quarks and antiquarks in the $c\bar{c}$ pair are almost uncorrelated in the azimuthal angle between them and are often produced in the configuration with quite large pair transverse momenta. The distributions may be different if one includes the kinematical cuts related to the experimental coverage of detectors and/or hadronization effects. Exact calculation of the absorptive corrections may also have some influence on the shapes of the distributions (especially for $\varphi_{c\bar{c}}$). However, in the moment, including them in a realistic manner is technically a difficult task and goes beyond the scope of this paper.

Figures 7 and 8 show the double differential cross sections as a functions of transverse momenta of incoming gluons (k_{1T} and k_{2T}) and transverse momenta of outgoing c and $\bar{c}$ quarks (p_{1T} and p_{2T}), respectively. We observe that quite large incident gluon transverse momenta enter into our calculations. The major part of the cross section is concentrated in the region of small k_t's of both gluons but long tails are present. Transverse momenta of the outgoing particles are not balanced as they are in the case of the LO collinear approximation. Such asymmetric configurations, where one p_t is small and the second one is large, correspond to the higher-order corrections in the collinear case and are also present in the k_t-factorization approach. Both pomeron and reggeon components give similar correlations in these planes.

JHEP02(2017)089

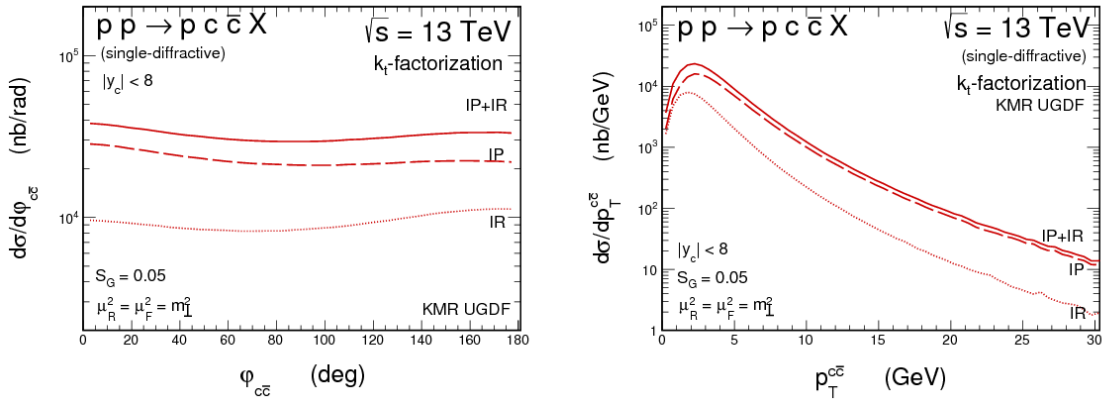

Figure 6. The distribution in $\phi_{c\bar{c}}$ (left panel) and distribution in $p_T^{c\bar{c}}$ (right panel) for k_t-factorization approach at $\sqrt{s} = 13\,\text{TeV}$.

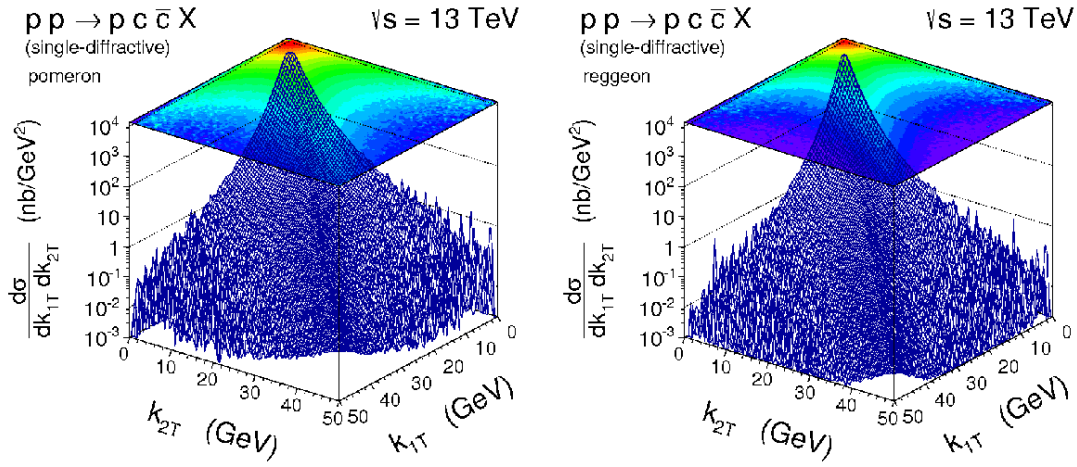

Figure 7. Double differential cross sections as a function of initial gluon transverse momenta k_{1T} and k_{2T} for single-diffractive production of charm at $\sqrt{s} = 13\,\text{TeV}$. The left and right panels correspond to the pomeron and reggeon exchange mechanisms, respectively.

In figure 9 we show a double differential cross section as a function of the transverse momenta of outgoing proton and incident gluon (on the pomeron side). Again we see quite large gluon transverse momenta, significantly larger than the one of the outgoing proton. The cross section is concentrated in the region of proton p_T smaller than 1 GeV. From the kinematics, the transverse momentum of the outgoing proton must be equal to the transverse momentum of the pomeron (or reggeon). This confirms that, in the first approximation, the pomeron (or reggeon) transverse momentum may be neglected and one can assume its zero-influence on the transverse momentum of the gluon emitted from the pomeron (or reggeon). For completeness this effect could be included in a future. We leave this for our future studies.

JHEP02(2017)089

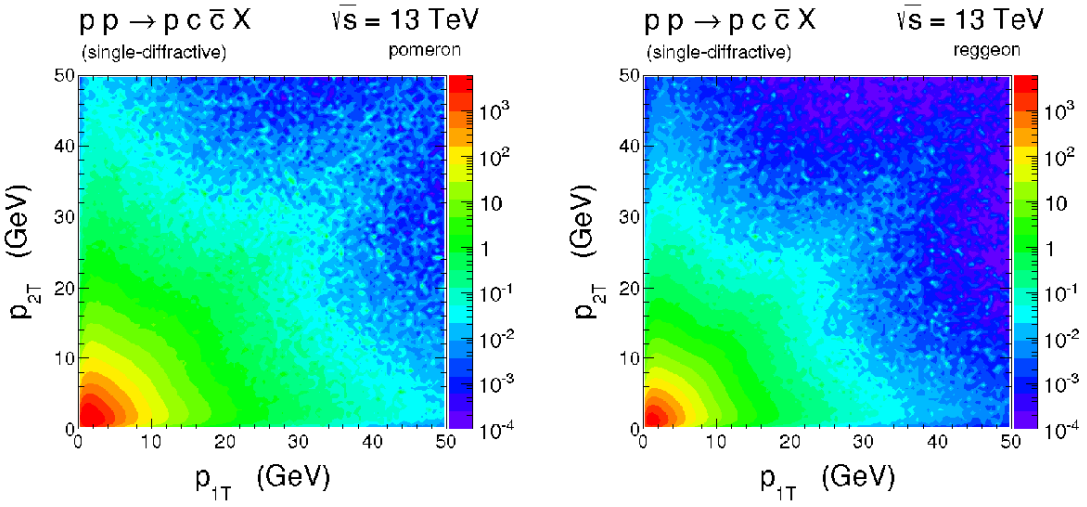

Figure 8. Double differential cross sections as a function of transverse momenta of outgoing c quark p_{1T} and outgoing $\bar{c}$ antiquark p_{2T} for single-diffractive production of charm at $\sqrt{s} = 13\,\text{TeV}$. The left and rights panels correspond to the pomeron and reggeon exchange mechanisms, respectively.

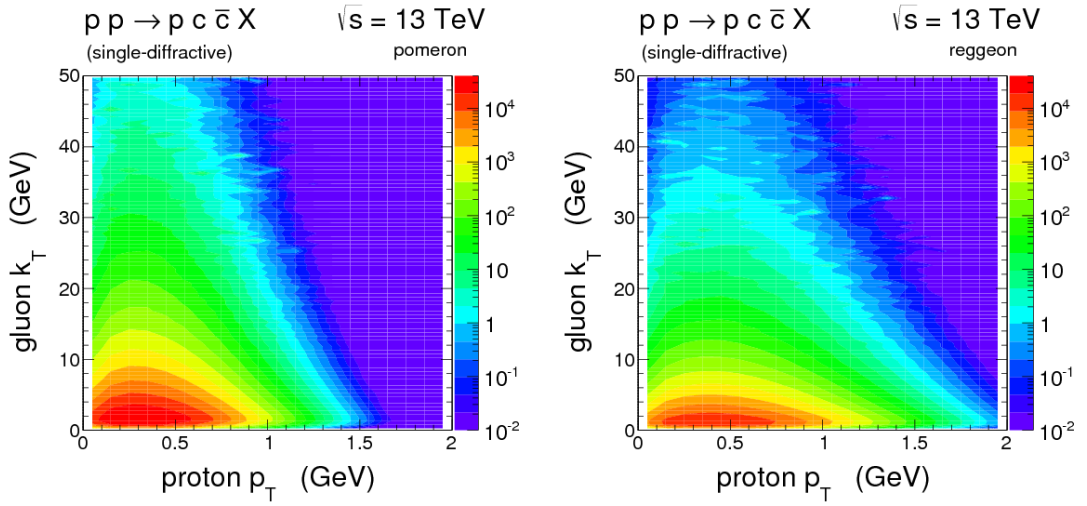

Figure 9. Double differential cross sections as a function of p_T of outgoing proton and k_T of incident gluon for the single-diffractive production of charm at $\sqrt{s} = 13\,\text{TeV}$. The left and right panels correspond to the pomeron and reggeon exchange mechanisms, respectively.

Figure 10 shows double differential cross sections as a function of p_T of outgoing proton and longitudinal momentum fraction of pomeron x_{IP} (left panel) and reggeon x_{IR} (right panel). The maxima of the cross sections for pomeron and reggeon contributions are concentrated in different regions of longitudinal momentum fractions. The pomeron contribution is strongly peaked at very small x_{IP}'s while the reggeon component rises when going to larger x_{IR}'s. However, the observed differences are not enough to show a clear way for experimental separation of the both mechanisms. Similar conclusions were obtained in the case of our former studies based on the collinear approach [28].

JHEP02(2017)089

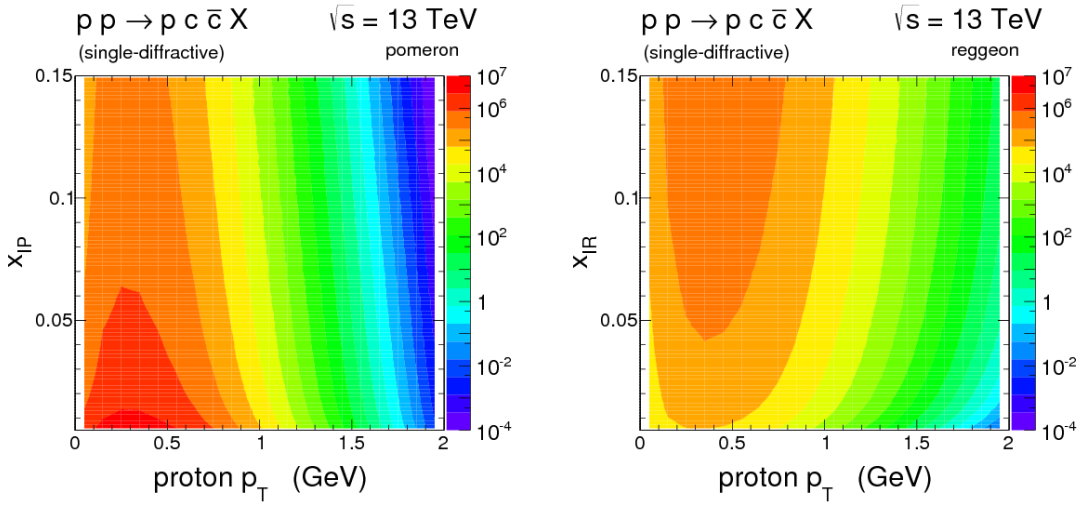

Figure 10. Double differential cross sections as a function of p_T of outgoing proton and longitudinal momentum fraction of the pomeron x_{IP} (left panel) and of the reggeon x_{IR} (right panel) for single-diffractive production of charm at $\sqrt{s} = 13\,\text{TeV}$.

Now we pass to the experimentally more motivated case of charm meson production. In figure 11, as an example, we present theoretical predictions for a single-diffractive production of D^0 meson at the LHC. Here the $c \to D$ hadronization effects were taken into account with the help of the standard Peterson fragmentation function (for more details see e.g. [29]). The fragmentation function is normalized with the experimentally well-known fragmentation fraction $\text{BR}(c \to D^0) = 0.565$. From the different species of D mesons the pseudoscalar neutral ones are produced most frequently. Here we concentrate on the ATLAS detector acceptance so the relevant cuts $p_t^D > 3.5\,\text{GeV}$ and $|\eta^D| < 2.1$ are applied. Both, pomeron and reggeon contributions are shown separately and the latter is found to be non-negligible, of the order of $\frac{IP}{IP+IR} \approx 20\%$. The relative reggeon contribution may be further slightly enhanced by increasing the lower limit of the x_{IP}, x_{IR} but this will also result in a some (factor 2–3) reduction of the overall visible cross section. Within the full acceptance, the integrated cross section for the ATLAS detector is predicted at the level of $3 - 4$ μb which is quite large. However, for a more definite conclusion whether the single-diffractive production of charm can be measured or not, a detailed feasibility studies are needed and are presented in section 5.

4 Towards phase space dependent gap survival factor

In the calculations presented in this paper the gap survival was taken to be a constant (small) value. Such values were typically obtained by two groups: Khoze-Martin-Ryskin (KMR) [2] and Gotsman-Levin-Maor (GLM) [3], calculating average (!) gap survival factor in soft single-diffractive processes. It is not clear whether such a value is relevant for our case. In principle, the gap survival factor may depend on several kinematical variables. To our knowledge this issue was not yet seriously discussed in the literature, especially in the context of hard single-diffractive production, as it is in our case.

JHEP02(2017)089

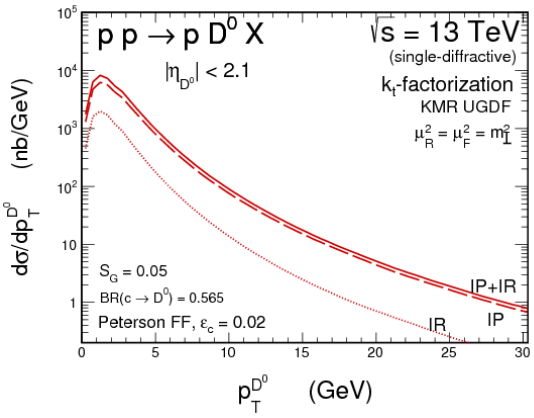

Figure 11. Transverse momentum distribution of D^0 meson within the ATLAS acceptance for single-diffractive production calculated within the k_t-factorization approach. Details are specified in the figure legend and in the text.

The dependence of the gap-survival factor on kinematical variables was calculated only for purely exclusive reactions. Our group has some experience in this context (see [33, 34] as typical examples).

It was shown that in exclusive reactions, as $pp \to pp\pi^+\pi^-$ for instance, the gap survival factor strongly depends only on t_1 and t_2 variables. Similar observation was made e.g. for the $pp \to ppJ/\Psi$ reaction [35]. The numerical effect depends therefore on whether the pomeron or photon is exchanged. We have checked that there is only very mild dependence of the gap survival factor on invariant mass of the created system and other variables.

The semi-exclusive single-diffractive reactions are paradoxically more difficult (bigger number of objects involved than in purely exclusive reactions). We wish to consider here a first toy model which may have some relevance for the case of interest. We start from the known to us case of exclusive production. How we proceed to the semi-exclusive case is sketched in figure 12. In our case of interest there is only one pomeron exchange instead of two pomeron exchanges for the $pp \to pp\pi^+\pi^-$ process. Therefore we replace the second pomeron exchange in exclusive case by a fictitious interaction with a steep t_2 dependence. Here we are only interested in the dependence of the gap survival factor on t_1, therefore it is enough to consider the ratio of cross section when including absorption effects and the cross section when neglecting absorption effects. The absorption effects are calculated as in ref. [33]. The strength of the coupling of the extra pomeron (leading to absorption) to proton and or proton remnant is kept the same as in ref. [33]. The coupling relevent for the energy considered here is taken.

In figure 13 we show the resulting gap survival factor as a function of t (t_1 in our toy model) (left panel) and invariant mass of the $c\bar{c}$ system (right panel). In obtaining this result we have checked that the slope of the t_2 dependence of the fictitious exchange practically does not influence this effect. We get $S_G \approx 0.1$ or even less at low t_1. In contrast, at larger t_1 we get even an enhancement. Similar enhancement was obtained in ref. [33] where it was even consistent with the corresponding experimental data for $pp \to pp\pi^+\pi^-$

JHEP02(2017)089

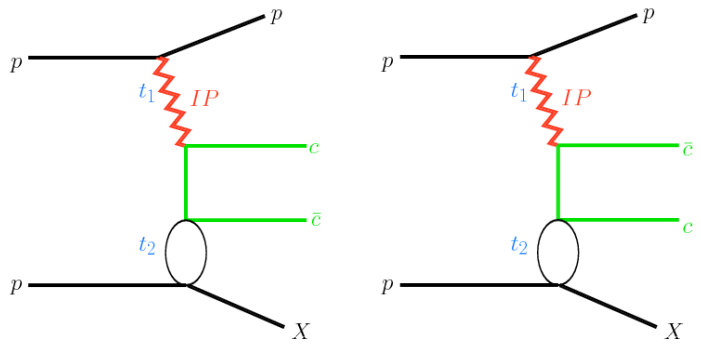

Figure 12. A diagrammatic representation of the toy model for semiexclusive production of $c\bar{c}$. The left and right diagrams are for t- and u-channels, respectively.

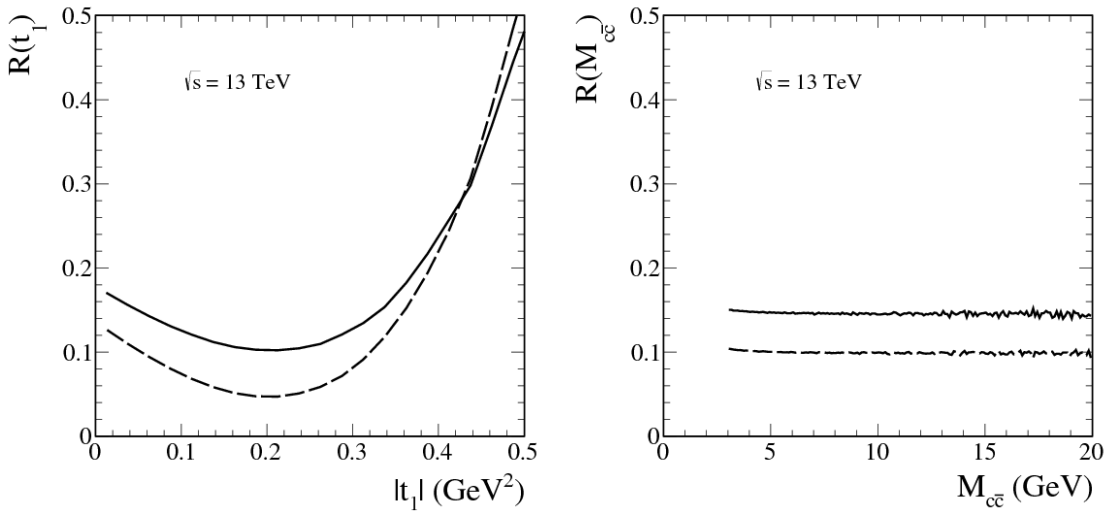

Figure 13. Gap survival factor as a function of $t = t_1$ (left panel) and $M_{c\bar{c}}$ (right panel). The result was obtained in the toy model sketched in figure 12. The slope of the pomeron exchange was fixed to $B = 4\,\mathrm{GeV}^{-2}$, which corresponds to the coupling of pomeron to $c/\bar{c}$ quarks/antiquarks. The slope of the fictitious interaction was taken to be $B = 10\,\mathrm{GeV}^{-2}$ (dashed line) and $B = 20\,\mathrm{GeV}^{-2}$ (solid line).

reaction. In contrast to the t distribution there is practically no dependence of gap survival factor on $M_{c\bar{c}}$ (see the right panel of figure 13).

The obtained here gap survival factor could, in principle, be used to roughly correct $d\sigma/dt$ of the scattered protons for our single-diffractive production of charm. Such a distribution could be accessible experimentally only when measuring forward protons. This will be hopefully the case in a future. For all other distributions presented in the present paper it is enough to multiply them by a constant gap survival factor.

Clearly it is very first attempt to estimate absorption effects for the considered reaction. More theoretical effort is required.

An alternative approach to gap survival and factorization breaking is to implement multiple interactions (MPI) in Monte Carlo event generators. These models are typically

JHEP02(2017)089

based on the eikonalization of the partonic cross section in hadronic collisions. According to this concept, any additional partonic scattering results in a colour exchange that would destroy a rapidity gap required in diffractive events. Some time ago PYTHIA has been used to calculate gap survival probability for exclusive Higgs boson production [36]. This analyses open a possibility to compare both approaches. As it turns out, the values predicted by PYTHIA are numerically in good agreement with those calculated in the standard approach by the KMR and GLM groups [4].

Very recently, the dynamic gap survival method has been incorporated in PYTHIA [37]. This unique tool opens a new possibility to extend our limited understanding of the effects associated with diffractive production. However, the treatment of the MPI's in the diffractive case is not clear and has large uncertainties. For our purposes, we have checked only that in the case of reaction considered in this paper, there is no t-dependence of the dynamical gap survival probability so one can use one global factor. The question is, however, very interesting, still open, and requires further theoretical engagement.

5 Feasibility studies

The predictions described in this paper can be verified experimentally using the LHC data. The characteristic signatures of a charm meson production in a single-diffractive mode are: large rapidity gap and scattered proton. The former one can be used by the LHCb experiment which has a good acceptance in the forward region. The latter, discussed in detail in the following section, can be used by ATLAS and CMS/TOTEM as these experiments are equipped with a special forward proton detectors.

Diffractive protons are usually scattered at very low angles, i.e. they are produced into the LHC beamline, thus cannot be measured. In order to measure them dedicated detectors, located in the LHC beam pipe hundreds of meters away from the interaction point, are needed. At the LHC there are two sets of such detectors: TOTEM/CT-PPS [38] installed around CMS interaction point and ALFA [39] and AFP [40] which are a part of the ATLAS experiment. The studies presented in this section focus on the ATLAS detectors, but very similar results are expected for the CMS/TOTEM case.

Charmed mesons are identified using tracks reconstructed by the ATLAS inner detector. Diffractive signature is due to the forward proton tag. Taking this into account, there are two main sources of background: soft single-diffractive and non-diffractive production. The presence of forward proton in the latter case is usually due to the pile-up — a situation, in which there are more than one interaction during a bunch-crossing. Therefore rather low pile-up runs are required.

Events with charmed mesons may be triggered using items sensitive to charged particles. Due to the minimum-bias backgrounds it is desirable to have a possibility of defining minimal transverse momentum in the trigger chain. In case of the ATLAS detector, the triggering can be done by requiring at least two hits in the Minimum Bias Scintillators or reconstructed track with p_T above a given threshold in inner tracking detectors.

JHEP02(2017)089

5.1 Charm meson reconstruction

Studies performed below are similar to the ones done by ATLAS (see ref. [41]). In the following, as an example, the production of $D^{*\pm}$ charmed mesons (hereafter called *signal)* is discussed. However, it is worth stressing that the production of $D^{\pm}$ and $D_s^{\pm}$ is also feasible. Predictions are based on events generated accordingly to the theoretical calculations described earlier in this paper. In these studies hadronization of charm and anti-charm quarks was done using Pythia 8 [42].

The response of the ATLAS detector was mimicked by applying a Gaussian smearing of $0.03 \otimes p_T$ in transverse momentum, 0.03 in pseudorapidity and 0.02 rad in azimuthal angle for each stable particle. These values are conservative and based on the performance studies published in [43] and [44]. In order to illustrate the detection efficiency, each track had a 85% chance of being reconstructed (see e.g. ref. [45]). The reconstruction efficiency of forward proton detectors was set to 95% [40].

The $D^{*\pm}$ mesons were identified in $D^{*\pm} \to D^0\pi^{\pm} \to (K^-\pi^+)\pi^{\pm}$ decay channel. For each signal and background event, all pairs of oppositely-charged tracks, each with $p_T > 1.0\,\text{GeV}$, were combined to form D^0 candidates. The decay length of the D^0 meson, calculated as the transverse distance between the candidate vertex and the primary vertex projected along the total transverse momentum of the track pair, was required to be greater than zero. The vertex reconstruction resolution of 300 μm was used [44]. In order to calculate the D^0 invariant mass, kaon and pion masses were assumed in turn for each track. In order to pass selection, events were required to be within $1.82 < M(D^0) < 1.91\,\text{GeV}$ mass window. Finally, $D^{*\pm}$ meson candidates were reconstructed in the range of transverse momentum $p_T^D > 3.5\,\text{GeV}$ and pseudorapidity $|\eta^D| < 2.1$. The background was reduced by requiring $p_T^D/E_T > 0.02$, where E_T is a sum of the transverse energy of stable particles (except neutrinos) generated within the range of the ATLAS calorimeter ($|\eta| < 4.9$).

After the selection described above, a clear signal is visible (see figure 14) in the region of $0.144 < \Delta M < 0.148$, where $\Delta M = M(K\pi\pi) - M(K\pi)$ is a difference between the mass of $D^{*\pm}$ and D^0 meson. The figure was done for relatively small pile-up intensity value of $\mu = 0.5$.

5.2 Forward protons

Due to the presence of the LHC magnets between the interaction point and the forward proton detectors, the proton trajectory is not a straight line. Obviously, it depends on the settings of the magnetic field. In the simplest way, such settings, called *optics*, could be characterized by the value of the betatron function at the interaction point, β^*. In the following, two optics at which the ATLAS forward detectors could take data are considered: $\beta^* = 0.55$ m and $\beta^* = 90$ m. Their properties are described in details in ref. [46] and their choice is justified in ref. [47].

The scattered protons were assumed to be measured in the forward detectors: ALFA and AFP. Together with two considered optics, this means four different experimental conditions. The geometric acceptance for these cases is widely discussed in detail in ref. [47].

JHEP02(2017)089

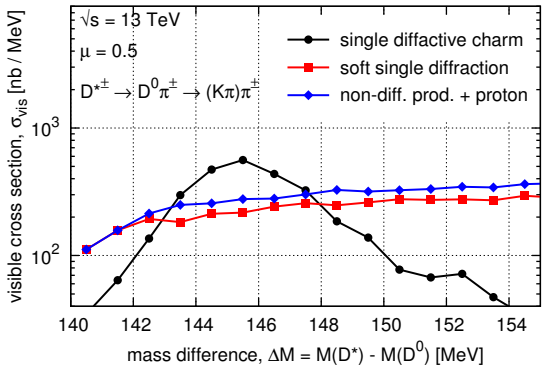

Figure 14. Visible cross section after the event selection as a function of mass difference between $D^{*\pm}$ and D^0 mesons. The black line is for signal whereas the red(blue) ones for single(non-) diffractive background. The pile-up intensity value was set to $\mu = 0.5$.

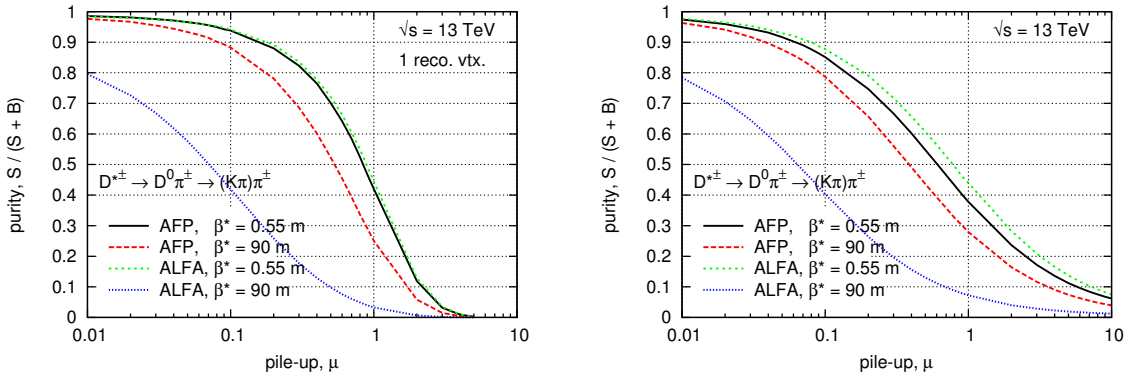

Figure 15. Sample purity as a function of pile-up intensity. The left panel shows situation with and the right panel without single vertex requirement (see text).

Protons were transported to the location of forward detectors using parametrised transport [48] trained on the relevant LHC optics [46]. Protons were checked to not be lost in the LHC aperture and to be within the detector active area. The beam-detector distance was set as in ref. [47].

The purity, defined as a ratio of signal (S) to the sum of signal and background ($S+B$) events, is shown in figure 15. The left(right) figure is for the situation with(without) single vertex requirement. Smaller purity for the case of the ALFA detector and $\beta^* = 90$ m optics is due to the protons scattered elastically. An additional anti-elastic selection (cf. ref. [49]) should improve the results.

In order to increase purity in the low pile-up data taking conditions, events with only one reconstructed vertex were considered. As is discussed in ref. [47], such a selection will greatly reduce the combinatorial, non-diffractive background.

JHEP02(2017)089

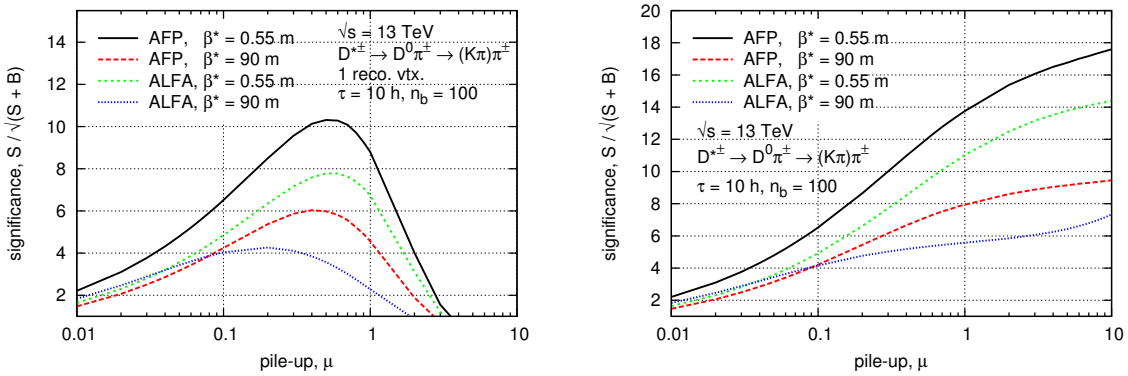

Figure 16. Statistical significance for 10 hours of data-taking with 100 bunches as a function of pile-up intensity μ. The left panel shows situation with and the right panel without single vertex requirement.

5.3 Results

The quality of the measurement can be expressed in terms of the statistical significance defined as $\frac{S}{\sqrt{S+B}}$. The results for all considered scenarios and the data-taking time of 10 hours with 100 colliding bunches as a function of pile-up is shown in figure 16. Again, the left(right) figure is for the selection with(without) single vertex requirement.

As can be concluded from the above figures, pure and significant measurement can be performed for a wide range of experimental conditions (mean pile-up, $0.05 < \mu < 1$). As expected, a single vertex requirement improves the purity for $\mu \lesssim 1$. For data taken with $\mu > 1$ the purity of the sample will be low, but the presence of the signal should be evident.

6 Conclusions

Charm production is a good example where the higher-order QCD effects play an important role. For the inclusive charm production we have shown that these effects can be effectively included in the k_t-factorization approach [29]. In the present paper we have presented a first application of the k_t-factorization to the hard single-diffractive production.

In our approach we decided to use the so-called KMR method to calculate diffractive unintegrated gluon distribution. As usually in the KMR approach, we have calculated diffractive gluon UGDFs based on collinear distribution, which here is the diffractive collinear gluon distribution. In our calculations we have used the H1 Collaboration parametrization of gluon distributions fitted to the HERA data on diffractive structure function and di-jet production.

Having obtained unintegrated diffractive gluon distributions we have performed calculations of several single-particle and correlation distributions. The results have been compared with the results of the leading-order collinear approximation. In general, the k_t-factorization approach leads to larger cross sections. However, the K-factor is strongly dependent on phase space point. We expect that our new predictions are better than the previous ones obtained in the collinear approach. Some correlation observables, like az-

JHEP02(2017)089

imuthal angle correlation between c and $\bar{c}$, and $c\bar{c}$ pair transverse momentum have been calculated for the first time.

The obtained cross sections for diffractive production of charmed mesons are fairly large and one could measure them. Such a measurement should give a chance not only to better understand the underlying mechanism of diffractive charm production but also the diffractive production in general. Therefore, we have supplemented our theoretical studies by a feasibility ones. The feasibility study of diffractive production of charm was done using forward proton spectrometers installed by the ATLAS and TOTEM collaborations at the LHC. These experiments should be able to measure $D^{*\pm}$, $D^{\pm}$ and $D_s^{\pm}$ charmed mesons produced with diffractively scattered proton. Taking the example of $D^{*\pm}$ production, we have shown that after the signal selection, a pure and significant measurement is expected to be doable for a wide range of experimental conditions ($0.05 < \mu < 1$).

In future, other unintegrated diffractive parton distributions can be calculated in an analogous way (KMR method) as for gluons. Such a new distributions could be used for other hard diffractive processes. This would open a new situation in studying hard diffractive processes. Several useful correlation observables would become accessible with this technology. A next step would be e.g. diffractive production of di-jets. For gauge boson production one could try to discuss transverse momentum distributions of gauge bosons as was done for the inclusive case. Clearly, new perspectives are now open.

So far there is only one measurement for single-diffractive production of charmed mesons [50]. The Fermilab data was a fixed target diffractive charm production for low energy ($\sqrt{s} = 40\,\mathrm{GeV}$), where the high-energy dipole approach with high-energy parametrization of dipole-proton cross section obtained fro the analysis of HERA data may be (at this low energies) too approximate. We have checked that our (resolved pomeron) approach gives cross section similar to the "experimental one". In fact the "experimental" in this case means a crude extrapolation from a limited corner of the phase space (limited range of x_F) for D^* mesons to the full phase space based on the resolved pomeron (Ingelman-Schlein) model. Also in our model the extrapolation to low energies is not very sure. Therefore we did not take seriously the quasi data. We hope real data may be obtained only now at the LHC and therefore we have presented relevant feasibility studies. We have presented several differential distributions that can be verified at the LHC. This would allow potentially also negative verification. In contrast, only total cross sections were presented in the dipole approach so far so its experimental verification may be difficult. In our opinion, comparing to only total cross section extrapolated in a model dependent way to the full phase space is rather risky.

Acknowledgments

We are indebted to Piotr Lebiedowicz for help in obtaining gap survival functions in our toy model. This study was partially supported by the Polish National Science Centre grants DEC-2013/09/D/ST2/03724 and DEC-2014/15/B/ST2/02528. Work of M.T. was partially supported by the Polish National Science Centre Mobility+ programme number 1285/MOB/IV/2015/0.

JHEP02(2017)089

Open Access. This article is distributed under the terms of the Creative Commons Attribution License (CC-BY 4.0), which permits any use, distribution and reproduction in any medium, provided the original author(s) and source are credited.

References

[1] G. Ingelman and P.E. Schlein, *Jet Structure in High Mass Diffractive Scattering*, *Phys. Lett.* **B 152** (1985) 256 [INSPIRE].

[2] V.A. Khoze, A.D. Martin and M.G. Ryskin, *Soft diffraction and the elastic slope at Tevatron and LHC energies: A MultiPomeron approach*, *Eur. Phys. J.* **C 18** (2000) 167 [hep-ph/0007359] [INSPIRE].

[3] E. Gotsman, E. Levin and U. Maor, *The Survival probability of large rapidity gaps in a three channel model*, *Phys. Rev.* **D 60** (1999) 094011 [hep-ph/9902294] [INSPIRE].

[4] E. Gotsman, E. Levin, U. Maor, E. Naftali and A. Prygarin, *Survival probability of large rapidity gaps*, hep-ph/0511060 [INSPIRE].

[5] L. Alvero, J.C. Collins, J. Terron and J.J. Whitmore, *Diffractive production of jets and weak bosons and tests of hard scattering factorization*, *Phys. Rev.* **D 59** (1999) 074022 [hep-ph/9805268] [INSPIRE].

[6] K. Golec-Biernat, C. Royon, L. Schoeffel and R. Staszewski, *Electroweak vector boson production at the LHC as a probe of mechanisms of diffraction*, *Phys. Rev.* **D 84** (2011) 114006 [arXiv:1110.1825] [INSPIRE].

[7] A. Cisek, W. Schafer and A. Szczurek, *Production of Z0 bosons with rapidity gaps: Exclusive photoproduction in gamma p and pp collisions and inclusive double diffractive Z0's*, *Phys. Rev.* **D 80** (2009) 074013 [arXiv:0906.1739] [INSPIRE].

[8] M. Klasen and G. Kramer, *Survival probability for diffractive dijet production in $p\bar{p}$ collisions from next-to-leading order calculations*, *Phys. Rev.* **D 80** (2009) 074006 [arXiv:0908.2531] [INSPIRE].

[9] A.K. Kohara and C. Marquet, *Prompt photon production in double-Pomeron-exchange events at the LHC*, *Phys. Lett.* **B 757** (2016) 393 [arXiv:1509.05551] [INSPIRE].

[10] C. Marquet, C. Royon, M. Saimpert and D. Werder, *Probing the Pomeron structure using dijets and γ+jet events at the LHC*, *Phys. Rev.* **D 88** (2013) 074029 [arXiv:1306.4901] [INSPIRE].

[11] G. Kubasiak and A. Szczurek, *Inclusive and exclusive diffractive production of dilepton pairs in proton-proton collisions at high energies*, *Phys. Rev.* **D 84** (2011) 014005 [arXiv:1103.6230] [INSPIRE].

[12] B. Kopeliovich, *Diffractive production of Drell-Yan pairs and heavy flavors*, *Phys. Lett.* **B 447** (1999) 308 [INSPIRE].

[13] M. Luszczak, A. Szczurek and C. Royon, *W^+W^- pair production in proton-proton collisions: small missing terms*, *JHEP* **02** (2015) 098 [arXiv:1409.1803] [INSPIRE].

[14] M. Luszczak, R. Maciula and A. Szczurek, *Subdominant terms in the production of $c\bar{c}$ pairs in proton-proton collisions*, *Phys. Rev.* **D 84** (2011) 114018 [arXiv:1109.5930] [INSPIRE].

[15] V.P. Goncalves, C. Potterat and M.S. Rangel, *Bottom production in Photon and Pomeron – induced interactions at the LHC*, *Phys. Rev.* **D 93** (2016) 034038 [arXiv:1511.07688] [INSPIRE].

JHEP02(2017)089

[16] ATLAS collaboration, *Rapidity gap cross sections measured with the ATLAS detector in pp collisions at* $\sqrt{s} = 7$ *TeV*, *Eur. Phys. J.* **C 72** (2012) 1926 [arXiv:1201.2808] [INSPIRE].

[17] ATLAS collaboration, *Studies of Diffractive Enhanced Minimum Bias Events in ATLAS*, ATLAS-CONF-2010-048 (2010).

[18] CMS collaboration, *Measurement of diffraction dissociation cross sections in pp collisions at* $\sqrt{s} = 7$ *TeV*, *Phys. Rev.* **D 92** (2015) 012003 [arXiv:1503.08689] [INSPIRE].

[19] CDF collaboration, F. Abe et al., *Observation of diffractive W boson production at the Tevatron*, *Phys. Rev. Lett.* **78** (1997) 2698 [hep-ex/9703010] [INSPIRE].

[20] D0 collaboration, V.M. Abazov et al., *Observation of diffractively produced W and Z bosons in* $\bar{p}p$ *collisions at* $\sqrt{s} = 1800$ *GeV*, *Phys. Lett.* **B 574** (2003) 169 [hep-ex/0308032] [INSPIRE].

[21] CDF collaboration, T. Affolder et al., *Diffractive dijets with a leading antiproton in* $\bar{p}p$ *collisions at* $\sqrt{s} = 1800$ *GeV*, *Phys. Rev. Lett.* **84** (2000) 5043 [INSPIRE].

[22] CDF collaboration, D. Acosta et al., *Diffractive dijet production at* $\sqrt{s} = 630$ *GeV and 1800 GeV at the Fermilab Tevatron*, *Phys. Rev. Lett.* **88** (2002) 151802 [hep-ex/0109025] [INSPIRE].

[23] ATLAS collaboration, *Dijet production in* $\sqrt{s} = 7$ *TeV pp collisions with large rapidity gaps at the ATLAS experiment*, *Phys. Lett.* **B 754** (2016) 214 [arXiv:1511.00502] [INSPIRE].

[24] CMS collaboration, *Observation of a diffractive contribution to dijet production in proton-proton collisions at* $\sqrt{s} = 7$ *TeV*, *Phys. Rev.* **D 87** (2013) 012006 [arXiv:1209.1805] [INSPIRE].

[25] B.Z. Kopeliovich, I.K. Potashnikova, I. Schmidt and A.V. Tarasov, *Diffractive Excitation of Heavy Flavors: Leading Twist Mechanisms*, *Phys. Rev.* **D 76** (2007) 034019 [hep-ph/0702106] [INSPIRE].

[26] W. Schäfer and A. Szczurek, *Low mass Drell-Yan production of lepton pairs at forward directions at the LHC: a hybrid approach*, *Phys. Rev.* **D 93** (2016) 074014 [arXiv:1602.06740] [INSPIRE].

[27] M. Łuszczak, W. Schäfer and A. Szczurek, *Diffractive dissociation of gluons into heavy quark-antiquark pairs in proton-proton collisions*, *Phys. Lett.* **B 729** (2014) 15 [arXiv:1305.4727] [INSPIRE].

[28] M. Łuszczak, R. Maciuła and A. Szczurek, *Single- and central-diffractive production of open charm and bottom mesons at the LHC: theoretical predictions and experimental capabilities*, *Phys. Rev.* **D 91** (2015) 054024 [arXiv:1412.3132] [INSPIRE].

[29] R. Maciuła and A. Szczurek, *Open charm production at the LHC — k_t-factorization approach*, *Phys. Rev.* **D 87** (2013) 094022 [arXiv:1301.3033] [INSPIRE].

[30] M.A. Kimber, A.D. Martin and M.G. Ryskin, *Unintegrated parton distributions*, *Phys. Rev.* **D 63** (2001) 114027 [hep-ph/0101348] [INSPIRE].

[31] H1 collaboration, A. Aktas et al., *Measurement and QCD analysis of the diffractive deep-inelastic scattering cross-section at HERA*, *Eur. Phys. J.* **C 48** (2006) 715 [hep-ex/0606004] [INSPIRE].

[32] A.D. Martin, W.J. Stirling, R.S. Thorne and G. Watt, *Parton distributions for the LHC*, *Eur. Phys. J.* **C 63** (2009) 189 [arXiv:0901.0002] [INSPIRE].

JHEP02(2017)089

[33] P. Lebiedowicz and A. Szczurek, *Revised model of absorption corrections for the $pp \to pp\pi^+\pi^-$ process*, *Phys. Rev.* **D 92** (2015) 054001 [arXiv:1504.07560] [INSPIRE].

[34] P. Lebiedowicz and A. Szczurek, *Exclusive production of heavy charged Higgs boson pairs in the $pp \to ppH^+H^-$ reaction at the LHC and a future circular collider*, *Phys. Rev.* **D 91** (2015) 095008 [arXiv:1502.03323] [INSPIRE].

[35] W. Schäfer and A. Szczurek, *Exclusive photoproduction of J/ψ in proton-proton and proton-antiproton scattering*, *Phys. Rev.* **D 76** (2007) 094014 [arXiv:0705.2887] [INSPIRE].

[36] L. Lönnblad and M. Sjodahl, *Uncertainties on central exclusive scalar luminosities from the unintegrated gluon distributions*, *JHEP* **05** (2005) 038 [hep-ph/0412111] [INSPIRE].

[37] C.O. Rasmussen and T. Sjöstrand, *Hard Diffraction with Dynamic Gap Survival*, *JHEP* **02** (2016) 142 [arXiv:1512.05525] [INSPIRE].

[38] TOTEM collaboration, *Total cross-section, elastic scattering and diffraction dissociation at the Large Hadron Collider at CERN: TOTEM Technical Design Report*, CERN-LHCC-2004-002 (2013).

[39] P. Jenni et al., *ATLAS Forward Detectors for Measurement of Elastic Scattering and Luminosity*, CERN-LHCC-2008-004 (2008).

[40] ATLAS collaboration, *Technical Design Report for the ATLAS Forward Proton Detector*, CERN-LHCC-2015-009 (2015).

[41] ATLAS collaboration, *Measurement of $D^{*\pm}$, $D^{\pm}$ and $D_s^{\pm}$ meson production cross sections in pp collisions at $\sqrt{s} = 7$ TeV with the ATLAS detector*, *Nucl. Phys.* **B 907** (2016) 717 [arXiv:1512.02913] [INSPIRE].

[42] T. Sjöstrand, S. Mrenna and P.Z. Skands, *A Brief Introduction to PYTHIA 8.1*, *Comput. Phys. Commun.* **178** (2008) 852 [arXiv:0710.3820] [INSPIRE].

[43] ATLAS collaboration, *The ATLAS Experiment at the CERN Large Hadron Collider*, 2008 *JINST* **3** S08003 [INSPIRE].

[44] ATLAS collaboration, *Estimating Track Momentum Resolution in Minimum Bias Events using Simulation and K_s in $\sqrt{s} = 900$ GeV collision data*, ATLAS-CONF-2010-009 (2010).

[45] ATLAS collaboration, *Charged-particle distributions in pp interactions at $\sqrt{s} = 8$ TeV measured with the ATLAS detector*, *Eur. Phys. J.* **C 76** (2016) 403 [arXiv:1603.02439] [INSPIRE].

[46] M. Trzebiński, *Machine Optics Studies for the LHC Measurements*, *Proc. SPIE Int. Soc. Opt. Eng.* **9290** (2014) 929026 [arXiv:1408.1836] [INSPIRE].

[47] M. Trzebinski, R. Staszewski and J. Chwastowski, *On the Possibility of Measuring the Single-tagged Exclusive Jets at the LHC*, *Eur. Phys. J.* **C 75** (2015) 320 [arXiv:1503.00699] [INSPIRE].

[48] M. Trzebinski, R. Staszewski and J. Chwastowski, *LHC High $\beta*$ Runs: Transport and Unfolding Methods*, *ISRN High Energy Phys.* **2012** (2012) 491460 [arXiv:1107.2064] [INSPIRE].

[49] ATLAS collaboration, *Measurement of the total cross section from elastic scattering in pp collisions at $\sqrt{s} = 7$ TeV with the ATLAS detector*, *Nucl. Phys.* **B 889** (2014) 486 [arXiv:1408.5778] [INSPIRE].

[50] M.H.L.S. Wang et al., *Diffractively produced charm final states in 800-GeV/c p p collisions*, *Phys. Rev. Lett.* **87** (2001) 082002 [INSPIRE].

JHEP02(2017)089